

A PERTURBATION METHOD FOR INDEX DETECTION FOR LINEAR MATRIX PENCILS

HANNA BLAZHKO AND MICHAŁ WOJTYŁAK

ABSTRACT. Rigorous, non-asymptotic bounds for the Puiseux expansion of the eigenvalue at infinity are given. Error analysis is provided. Further, the expected value of the eigenvector condition number of a randomly perturbed matrix is estimated. The latter result is applied to the Cayley transform of the linear pencil. Numerical simulations illustrating the theoretical findings are provided.

1. INTRODUCTION

In recent years, significant progress has been made in randomized methods for computing eigenvalues of linear pencils, in particular for singular pencils [18, 19, 21] and singular quadratic polynomials [22], thereby overcoming the classical limitation [37]. These methods—based on random perturbations of a prescribed rank, random projections, and random augmentations—often demonstrate performance superior to that of the classical staircase algorithm [36]. While the new approach successfully determines the eigenvalues, it does not address the computation of the Kronecker form. The aim of the present work is to make progress in this direction. For simplicity, we restrict our attention to regular pencils, and on the *index*, i.e., the size of the largest Kronecker block associated with the eigenvalue at infinity. We also briefly indicate how the results on index can be transferred to finite eigenvalues. We refer to [9, 30, 29, 12] for applications of index 2 systems. While our work is pure finite-dimensional, it is also related to a recent infinite-dimensional study on index concepts, studied in detail in [10].

We approach the problem using the first-order perturbation theory developed in [24] and [8]. The latter paper states that for a pencil $\lambda E - A$ with an eigenvalue infinity with the largest Kronecker block of size k , the eigenvalues of the perturbed pencil

$$\lambda E - A + \tau(\lambda X - Y),$$

where $\lambda X - Y \in \mathbb{C}^{n \times n}[\lambda]$ is a generic perturbation, admit, for sufficiently small τ , a Puiseux expansion

$$\lambda(\tau) = C\tau^{-1/k} + o(\tau^{-1/k}) \tag{1.1}$$

with some constant $C \neq 0$. Our idea is to use this expansion to determine the index. However, recall that the numerical algorithms tend to replace the Kronecker blocks of size k by k single eigenvalues in the neighborhood of λ_0 , see, e.g., [1, 3, 32, 34]. Hence, the first question that needs to be posed for applying the method follows:

(Q1) *Can the fractional expansion (1.1) be observed in numerical simulations?*

Rephrasing the question, we are interested in whether a small perturbation $\Delta(\lambda)$ of $\lambda E - A$ leads to a corresponding perturbation of the behavior described by (1.1). We give a positive answer to this question, providing (in case $k = 2$) a rigorous non-asymptotic estimate $C_1\tau^{-1/2} \leq |\lambda_\Delta(\tau)| \leq C_2\tau^{-1/2}$ of the eigenvalue $\lambda_\Delta(\tau)$ of the perturbed pencil. The next question we address is

(Q2) *Is the same behavior observed in the discretization?*

For that, we consider the simplest discretization model, given by the Cayley transform of the pencil,

$$(E - hA)^{-1} (E + hA).$$

In our approach, we perturb this matrix with a random matrix and average the results over several samples (see below for details). Our theoretical results here are based on a recent technique [6] that allows controlling the eigenvector condition number of the perturbed matrix. This allows us to give a positive answer to the second question. This leads to the third, central objective:

(Q3) *Can the observed behavior of the perturbed eigenvalues be used to determine the index?*

Our theoretical and numerical results confirm that it is possible to determine whether a given pencil lies in proximity to the set of index-two pencils. In this sense, our work can be seen as solving a distance problem, see (1.4) for details on the norm used. We refer here to [2, 4, 5, 14, 23], and [15, 27] for related distance problems for matrices and matrix pencils, respectively.

Although the theorems are formulated for general matrices, they are particularly suited for pencils connected with energy-based modeling. We refer the reader to [29] for an overview and to [15, 16, 17] for related distance problems. Several applications appear in Section 5. In particular, we discuss dissipative Hamiltonian pencils, i.e., pencils of the form $\lambda E - (J - R)Q$, where all matrices are complex square ones, satisfying additionally $E^*Q \geq 0$, $R \geq 0$, and $J = -J^*$. The Kronecker form of these pencils is described in [26, 27] and [11]. In Section 3, we contribute to the topic by discussing the case $Q > 0$. The remarkable property of such pencils is that all their eigenvalues lie in the closed left half-plane, and the eigenvalues on the imaginary axis are always semisimple, except possibly for a Kronecker block of size two at zero or at infinity. Notably, $R > 0$ implies index one, see [15]. On the other hand, Kronecker blocks of size one violate minimality of the system, see [12], which motivates the main assumption in Theorem 1.1 below and in subsequent corollaries. An additional motivation for (Q2) is that in this setting the Cayley transform is the basis for the implicit midpoint rule, one of the simplest discretization rules preserving the energy, cf. [20] for implementation for port-Hamiltonian system.

We discuss now the main results of the paper. We consider complex matrices with the euclidean norm. A central role in both the deterministic and probabilistic analyses is played by the *eigenvector condition number* defined as

$$\kappa_V(X) := \inf \{ \kappa(T) : T \in \mathbb{C}^{n,n}, T \text{ invertible}, T^{-1}XT \text{ diagonal} \},$$

where $\kappa(T) := \|T\| \cdot \|T^{-1}\|$ is the *condition number* of a matrix.

1.1. Deterministic results. The symbol $\sigma_{\min}(E)$ denotes the smallest singular value of E (possibly zero). Throughout, we also use

$$E_{11} := P_{\text{ran } E} E P_{\text{ran } E}, \quad A_{11} := P_{\text{ran } E} A P_{\text{ran } E}, \quad A_{12} := P_{\text{ran } E} A P_{\text{ker } E}, \quad A_{21} := P_{\text{ker } E} A P_{\text{ran } E}, \quad (1.2)$$

where $P_{\mathcal{X}} \in \mathbb{C}^{n,n}$ stands for the orthogonal projection onto a subspace \mathcal{X} of \mathbb{C}^n .

Furthermore, we define

$$\tau_0 := \sup \left\{ \tau \geq 0 : |\mu(\tau)| > \frac{\|A_{11}\|}{\tau + \sigma_{\min}(E_{11})/2} \text{ for some ev. } \mu(\tau) \text{ of } \lambda(E + \tau I) - A \right\}. \quad (1.3)$$

Note that $\tau_0 > 0$, provided that infinity is an eigenvalue of $\lambda E - A$, and $\tau_0 = \infty$ if, additionally, $A_{11} = 0$.

Theorem 1.1. *Let $\lambda E - A \in \mathbb{C}^{n,n}[\lambda]$ be a regular pencil of index two with no Kronecker blocks corresponding to infinity of size one and with $E \geq 0$. Then a perturbed pencil*

$$\lambda(E + \tau I + \Delta_E) - (A + \Delta_A), \quad \|\Delta_E\|, \|\Delta_A\| \leq \delta < \sigma_{\min}(E_{11}), \quad (1.4)$$

is regular and has an eigenvalue $\mu_{\Delta}(\tau)$ satisfying

$$\frac{1}{\sqrt{\tau}} \sqrt{\frac{\sigma_{\min}(A_{12}A_{21})}{\frac{3}{2}\|E_{11}\| + 2\tau}} - \gamma(\delta, \tau) \leq |\mu_{\Delta}(\tau)| \leq \frac{1}{\sqrt{\tau}} \sqrt{\frac{\|A_{12}A_{21}\|}{\frac{1}{2}\sigma_{\min}(E_{11})}} + \gamma(\delta, \tau), \quad (1.5)$$

where

$$\gamma(\delta, \tau) = \delta \cdot \kappa_V((E + \tau I)^{-1}A) \frac{\tau + \|A\|}{\tau(\tau - \delta)}, \quad 0 \leq \delta < \tau \leq \tau_0. \quad (1.6)$$

The formulation of Theorem 1.1 as stated above is optimal for general purposes. However, it can be refined with sharper estimates in certain special cases and extended in various ways to cover more general scenarios. In the following sections, we present several such adaptations tailored to our numerical experiments. For convenience, we summarize them here.

- The case $\delta = 0$ provides bounds on the leading coefficient in the Puiseux expansion in the index 2 case. Meanwhile, the case $\delta > 0$ shows how the numerical results deviate from the square-root bounds when the pencil is δ -close to an index-two pencil.
- Sharper estimates in the case $\Delta_E = 0$ and for dissipative Hamiltonian pencils are given in Corollary 2.2 and Corollary 3.3, respectively.
- Generalizations to a diagonalizable E and arbitrary E are given in Remark 2.3 and Remark 2.4, respectively.
- An extension to arbitrary finite eigenvalues of the pencil $\lambda E - A$ is discussed in Remark 2.5.

A limitation of Theorem 1.1 is the presence of the eigenvector condition number $\kappa_V((E + \tau I)^{-1}A)$ which may in principle be unbounded. We address this issue in two ways. First, in Section 3, we consider a special class of dissipative Hamiltonian pencils for which this condition number admits a sharper upper bound, see Corollary 3.3. Second, we replace the deterministic perturbation τI by probabilistic perturbations, allowing us to control the eigenvector condition number. This approach is discussed in more detail in the following subsection.

1.2. Probabilistic results. The second theoretical result of the paper is presented below. By a *complex Ginibre matrix* we understand an $n \times n$ random matrix $G_n = [g_{ij}]_{i,j=1}^n$ with i.i.d. complex Gaussian entries, i.e. with real and imaginary parts being independent $\mathcal{N}(0, 1/2n)$ random variables. Let M and Δ be two arbitrary matrices. Recall that for fixed $\tau > 0$ both matrices $M + \tau G_n$ and $M + \Delta + \tau G_n$ have n distinct eigenvalues with probability one. We denote them, respectively, by $\lambda_i(\tau)$ and $\lambda_i^{\Delta}(\tau)$, $i = 1, \dots, n$, $\tau > 0$. The ordering is not essential in what follows. The symbol \mathbb{E} denotes the expected value (with respect to the Ginibre matrix).

Theorem 1.2. *Let $M, \Delta \in \mathbb{C}^{n,n}$ be matrices with $\|M\|, \|M + \Delta\| \leq 1$. Then there exists a universal constant $\alpha(n)$, dependent only on the dimension n , such that*

$$\left| \mathbb{E} \min_{i=1, \dots, n} |\lambda_i^{\Delta}(\tau)| - \mathbb{E} \min_{i=1, \dots, n} |\lambda_i(\tau)| \right| \leq \frac{\alpha(n) \|\Delta\|}{\tau}, \quad \tau \in (0, 1). \quad (1.7)$$

Moreover, $\lim_{n \rightarrow \infty} \frac{\alpha(n)}{n^{3/2}} < 7.82843$.

In the subsequent sections, we apply this result to $M = \frac{M_h(E, A) + I}{\|M_h(E, A) + I\|}$, where

$$M_h(E, A) := [E - hA]^{-1} [E + hA]$$

for such $h \in \mathbb{R}$ that matrix $(E - hA)$ is invertible. Recall that if λ_0 is an eigenvalue of the pencil $\lambda E - A$ then $\mu_0 = \frac{1+h\lambda_0}{1-h\lambda_0}$ is an eigenvalue of $M_h(E, A)$, and the structure of the Kronecker blocks of

$\lambda E - A$ at λ_0 and the Jordan blocks of $M_h(E, A)$ at μ_0 coincide, see [25]. In particular, if $\lambda E - A$ has an eigenvalue ∞ of index 2 then, for τ in a neighborhood of 0, the perturbed matrix $M + \tau G_n$ has eigenvalues with expansion

$$\lambda(\tau) = C'\tau^{1/2} + o(\tau^{1/2}) \quad (1.8)$$

for some constant C' , depending on the sample of the random matrix. Theorem 1.2 estimates the deviation of this bound when perturbing M by a small norm matrix Δ .

1.3. Organization of the paper. Two main theorems have already been formulated above (Theorem 1.1 and Theorem 1.2). We continue with a detailed analysis of Theorem 1.1 in Section 2, therein one may find the full proof and corollaries mentioned above. In Section 3, we discuss the dissipative Hamiltonian setting. Section 4 is devoted to probabilistic reasoning constituting the proof of Theorem 1.2. Finally, in Section 5, we focus on practical aspects and compare both approaches through several simulations motivated by real-life examples.

2. THEOREM 1.1: AUXILIARY RESULTS, PROOF, AND COROLLARIES

First, we establish an auxiliary result.

Proposition 2.1. *Let $\lambda E - A$ be a pencil with $E \geq 0$. Then the following are equivalent:*

- (i) $\lambda E - A$ is regular of index at least two with no Kronecker blocks corresponding to infinity of size one;
- (ii) for some unitary matrix U one has $U^*(\lambda E - A)U$ of the form

$$\lambda \begin{bmatrix} E_{11} & 0 \\ 0 & 0 \end{bmatrix} - \begin{bmatrix} A_{11} & A_{12} \\ A_{21} & 0 \end{bmatrix}, \quad (2.1)$$

with A_{12} having full column rank, A_{21} having full row rank, E_{11} being diagonal and invertible, and the size of E_{11} being strictly less than the size of E .

Furthermore, if $A = J - R$ with $J = -J^*$ and $R \geq 0$ then U^*JU and U^*RU can be partitioned conformably with (2.1) as

$$U^*JU = \begin{bmatrix} J_{11} & J_{12} \\ -J_{12}^* & 0 \end{bmatrix}, \quad U^*RU = \begin{bmatrix} R_{11} & 0 \\ 0 & 0 \end{bmatrix}. \quad (2.2)$$

Proof. Assume (i) and let us take a diagonalisation U of E , such that

$$U^*EU = \begin{bmatrix} E_{11} & 0 \\ 0 & 0 \end{bmatrix}, \quad U^*AU = \begin{bmatrix} A_{11} & A_{12} \\ A_{21} & A_{22} \end{bmatrix},$$

with E_{11} invertible. For simplicity we can assume from now on that $U = I$. As ∞ is an eigenvalue of $\lambda E - A$, the size of E_{11} has to be strictly less than the size of E . Observe now that $A_{22} = 0$. Indeed, suppose the converse and let $A_{22}x_2 \neq 0$ for some $x_2 \neq 0$. Consider the vector $x = [0, x_2]^T$, partitioned conformably with (2.1). Observe that $x \in \ker E$, while there is no vector y satisfying $Ey = Ax$. Hence, in the Kronecker form of $\lambda E - A$ there is a simple Kronecker block corresponding to infinity, contradiction. Finally, since the pencil is regular, A_{12} has full column rank and A_{21} has full row rank, what finishes the proof of the forward implication.

To see the backward implication, notice that a pencil satisfying (ii) is clearly regular. By Lemma 3 of [27] it is of index at least 2. Note that there are no simple blocks corresponding to infinity as $A(\ker E) \subseteq \text{ran } E$.

To show (2.2), observe that $A_{22} = 0$ implies $J_{22} = R_{22} = 0$. As R is positive semidefinite, we have $R_{12} = 0$ and $R_{21} = 0$ as well. □

We prove now the main result. Observe that the eigenvalue condition number (see, e.g., [33]) is unsuitable for obtaining non-asymptotic bounds such as those provided in Theorem 1.1. The only available perturbation technique for tracking the fractional expansion under perturbation appears to be the eigenvector condition number together with the Bauer-Fike theorem. Although the bound obtained from such reasoning may initially seem pessimistic, in specific examples it provides quite accurate estimates of the range of τ for which the theorem holds true, see Subsection 5.5.

Proof of Theorem 1.1. First assume that $\delta = 0$. By Proposition 2.1 we may assume that the pencil is of the form (2.1). Fix $\tau \in (0, \tau_0)$, and let $\mu = \mu(\tau)$ be as in the definition of τ_0 , cf. (1.3). We show that it satisfies (1.5). Observe that $\eta = \frac{1}{\mu}$ is an eigenvalue of the reversal pencil $\lambda A - (E + \tau I)$, satisfying

$$\|A_{11}\| |\eta| < \tau + \sigma_{\min}(E_{11})/2. \quad (2.3)$$

This produces

$$\frac{1}{2} \sigma_{\min}(E_{11}) \|x\| \leq \|(E_{11} + \tau I - \eta A_{11})x\| \leq \left(\frac{3}{2} \|E_{11}\| + 2\tau\right) \|x\|, \quad x \in \mathbb{C}^{n_1}, \quad (2.4)$$

where $n_1 \times n_1$ is the dimension of E_{11} . In particular, the matrix $E_{11} + \tau I - \eta A_{11}$ is invertible. Hence, the Schur complement of the block matrix $\eta A - (E + \tau I)$,

$$\tau I - \eta^2 A_{21}(E_{11} + \tau I - \eta A_{11})^{-1} A_{12},$$

has to be singular. This, by the Woodbury matrix identity, implies the singularity of

$$\eta^2 A_{12} A_{21} - \tau(E_{11} + \tau I - \eta A_{11}).$$

The latter, in turn, implies that μ^2 is an eigenvalue of the regular linear pencil $A_{12} A_{21} - \lambda(\tau(E_{11} + \tau I - \eta A_{11}))$, and hence, also of the matrix

$$A_{12} A_{21} (\tau(E_{11} + \tau I - \eta A_{11}))^{-1}.$$

Thus,

$$\frac{\sigma_{\min}(A_{12} A_{21})}{\sigma_{\min}(\tau(E_{11} + \tau I - \eta A_{11}))} \leq \mu^2 \leq \|A_{12} A_{21}\| \|(\tau(E_{11} + \tau I - \eta A_{11}))^{-1}\|,$$

which, together with (2.4), finishes the proof of the inequality (1.5) in case $\gamma = 0$.

Now take arbitrary $\delta > 0$ and let $\delta < \tau < \tau_0$ and $\mu(\tau)$ be as in (1.3). Note that $\mu(\tau)$ is also an eigenvalue of the matrix $(E + \tau I)^{-1} A$, as $E + \tau I$ is positive (and hence, nonsingular). Observe that $E + \tau I + \Delta_E$ is nonsingular as well, due to $\delta < \tau$. Further, we have

$$S := (E + \tau I + \Delta_E)^{-1} (A + \Delta_A) = (E + \tau I)^{-1} A + \Delta,$$

with some matrix Δ satisfying a usual estimate

$$\|\Delta\| \leq \delta \cdot \frac{\tau + \|A\|}{\tau(\tau - \delta)}, \quad \text{for } \tau > \delta. \quad (2.5)$$

By the Bauer-Fike theorem [7] there exists an eigenvalue $\mu_\Delta(\tau)$ of S satisfying

$$|\mu(\tau) - \mu_\Delta(\tau)| \leq \gamma(\delta, \tau).$$

As the eigenvalues of S are also eigenvalues of the perturbed pencil $\lambda(E + \tau I + \Delta_E) - (A + \Delta_A)$, the proof is finished. \square

Corollary 2.2. *Let $E, A, \Delta_E, \Delta_A, \tau_0$ be as in Theorem 1.1, and assume in addition that $\Delta_E = 0$. Then inequality (1.5) holds with the sharper error bound on a larger set:*

$$\gamma(\delta, \tau) = \delta \frac{\kappa_V((E + \tau I)^{-1} A)}{\tau}, \quad 0 < \tau \leq \tau_0. \quad (2.6)$$

Proof. It suffices to observe that, in the case $\Delta_E = 0$, the estimate (2.5) in the proof of Theorem 1.1 improves to

$$\|\Delta\| \leq \frac{\delta}{\tau}, \quad \tau > 0.$$

□

Remark 2.3. If E is diagonalizable with nonnegative eigenvalues, then the statement of Theorem 1.1 holds with $\|X\|$, $\sigma_{\min}(X)$, $\kappa_V(X)$ ($X \in \mathbb{C}^{n,n}$), and orthogonal projections in formulas (1.2)–(1.6) understood with respect to the inner product $\langle x, y \rangle_T := y^* T^{-*} T^{-1} x$, ($x, y \in \mathbb{C}^n$), where T is a diagonalization of E . Indeed, observe that E is selfadjoint and nonnegative with respect to this new inner product and so Theorem 1.1 can be applied directly. It is informative to clarify the dependencies between the original matrix norm (minimal singular value, condition number, eigenvector condition number, respectively) and the corresponding quantities with respect to the inner product $\langle x, y \rangle_T$, which we denote with the subscript T . The following inequalities hold

$$\begin{aligned} \frac{1}{\kappa(T)} \|X\| &\leq \|X\|_T = \|T^{-1} X T\| \leq \|X\| \kappa(T), \\ \frac{1}{\kappa(T)} \sigma_{\min}(X) &\leq \sigma_{\min}(X)_T = 1 / \|X^{-1}\|_T \leq \sigma_{\min}(X) \kappa(T), \\ \kappa(X)_T &\leq \kappa(T)^2 \kappa(X), \\ \kappa_V(X)_T &= \inf\{\kappa(W)_T : W X W^{-1} \text{ is diagonal}\} \leq \kappa(T)^2 \kappa_V(X). \end{aligned}$$

Remark 2.4. Let $\lambda E - A \in \mathbb{C}^{n,n}[\lambda]$ be as in Theorem 1.1, with E arbitrary. Let $U \Sigma V^*$ be a singular value decomposition of E . To obtain similar bounds for expansions of eigenvalues, we may consider perturbation τUV^* instead of τI . Indeed, multiplying the pencil $\lambda(E + \Delta_E + \tau UV^*) - (A + \Delta_A)$ from the left by U^* and from the right by V we obtain a (strictly equivalent) pencil $\lambda(\Sigma + U^* \Delta_E V + \tau I) - (U^* A V + U^* \Delta_A V)$, to which we then can apply Theorem 1.1. The details are left to the reader.

Remark 2.5. Let λ_0 be a finite eigenvalue of the pencil $\lambda E - A$, and assume that $A - \lambda_0 E \geq 0$. To derive results analogous to Theorem 1.1, we first shift λ_0 to zero by considering the pencil $\lambda E - (A - \lambda_0 E)$. We then apply Theorem 1.1 to the reversal pencil $\lambda(A - \lambda_0 E) - E$. Let $\mu(\tau)$ denote the corresponding eigenvalues of $\lambda(A - \lambda_0 E + \tau I) - E$. It follows that the original perturbed pencil $\lambda E - (A + \tau I)$ has eigenvalues of the form $\lambda_0 + \frac{1}{\mu(\tau)}$. The corresponding estimates are then obtained by performing the same transformation on the inequalities in (1.5).

3. PORT-HAMILTONIAN PENCILS

As most our examples refer to this class of pencils, we devote the whole section to establish some properties crucial in their analysis. We are interested in matrix pencils of the form

$$\lambda E - (J - R)Q \in \mathbb{C}^{n,n}[\lambda], \quad J^* = -J, \quad Q^* E \geq 0, \quad R \geq 0, \quad \begin{array}{ll} \text{(a)} & Q \text{ invertible,} \\ \text{(b)} & Q > 0 \\ \text{(c)} & Q = I_n. \end{array} \quad (3.1)$$

Below we discuss the algebraic properties and highlight subtle differences between these choices of Q .

Theorem 3.1. *Assume that a pencil $\lambda E_0 - A_0$ is regular. Then*

- (i) $\lambda E_0 - A_0$ is of the form (3.1)(a) if and only if its eigenvalues are contained in the closed left half-plane, finite eigenvalues on the imaginary axis have Kronecker blocks of size one and the infinity has Kronecker blocks of size at most two.

- (ii) $\lambda E_0 - A_0$ is of the form (3.1)(b) if and only if for some invertible T we have $\lambda E_0 - A_0 = T^{-1}(\lambda E - (J - R))T$, where $\lambda E - (J - R)$ is of the form (3.1)(c). In particular, in such case E_0 is diagonalizable with nonnegative eigenvalues.

Proof. (i) The forward implication follows directly from [28, Thm.3.1]. To see the reverse implication observe that, again by [28, Thm.3.1], a pencil $\lambda E_0 - A_0$ enjoying the listed properties satisfies

$$\lambda E_0 - A_0 = S(\lambda E - (J - R))T, \quad E, R \geq 0, \quad J = -J^*,$$

with some invertible S, T , and $\lambda E - (J - R)$ of the form (3.1)(c). Setting $Q := S^{-*}T$, we obtain

$$\lambda E_0 - A_0 = \lambda SET + S(J - R)S^*Q, \quad Q^*(SET) = T^*ET \geq 0.$$

(ii) To see the forward implication set $T = Q_0^{-1/2}$, where $Q_0 \geq 0$ comes from the form (3.1)(b) of the pencil $\lambda E_0 - A_0$. Then, for $A_0 = J_0 - R_0$, we have

$$T^{-1}(\lambda E_0 - (J_0 - R_0)Q_0)T = \lambda Q_0^{1/2}E_0Q_0^{-1/2} - Q_0^{1/2}(J_0 - R_0)Q_0^{1/2},$$

which is clearly of the form (3.1)(c).

The backward implication follows by setting $Q = T^*T$. □

Remark 3.2. Statement (ii) reveals difficulties in characterizing pencils of the form (3.1) with $Q > 0$ in terms of the Kronecker form. Namely, it can be restated as saying that a given pencil is of the form (3.1) with $Q > 0$ if and only if it is similar to a pencil with the Kronecker form as in (i), with the similarity matrices S, T satisfying $S = T^{-1}$. Characterizing pencil equivalence with respect to the relation $L(\lambda) = T^{-1}P(\lambda)T$ is not feasible.

Next we restate Theorem 1.1 in the port-Hamiltonian setting, obtaining some further simplification. Recall that τ_0 was defined in (1.3), while E_{11} in (1.2).

Corollary 3.3. *Let $\lambda E - (J - R)Q \in \mathbb{C}^{n,n}[\lambda]$ be a regular pencil of the form (3.1) and of index two with no Kronecker blocks corresponding to infinity of size one.*

- (i) *If $Q = I$ then a perturbed pencil*

$$\lambda(E + \tau I + \Delta_E) - (A + \Delta_A), \quad \|\Delta_E\|, \|\Delta_A\| \leq \delta < \sigma_{\min}(E_{11}), \quad (3.2)$$

is regular and has an eigenvalue $\mu_{\Delta}(\tau)$ satisfying

$$\frac{1}{\sqrt{\tau}} \frac{\sigma_{\min}(J)}{\sqrt{\frac{3}{2}\|E\| + 2\tau}} - \gamma(\delta, \tau) \leq |\mu_{\Delta}(\tau)| \leq \frac{1}{\sqrt{\tau}} \frac{\|J\|}{\frac{1}{2}\sqrt{\sigma_{\min}(E_{11})}} + \gamma(\delta, \tau), \quad (3.3)$$

where

$$\gamma(\delta, \tau) = \delta \cdot \kappa_V((E + \tau I)^{-1}A) \frac{\tau + \|A\|}{\tau(\tau - \delta)}, \quad 0 \leq \delta < \tau < \tau_0. \quad (3.4)$$

Furthermore, in the case $R = 0$, the eigenvalue condition number admits the following estimate

$$\kappa_V((E + \tau I)^{-1}J) \leq \kappa(E + \tau I) \leq \frac{\|E\| + \tau}{\tau}. \quad (3.5)$$

- (ii) *For arbitrary $Q > 0$, the statements in (i) hold true with $\|X\|$, $\sigma_{\min}(X)$, $\kappa(X)$, $\kappa_V(X)$ ($X \in \mathbb{C}^{n,n}$), and τ_0 understood with respect to the inner product $\langle x, y \rangle_Q = \langle Qx, y \rangle$.*

Proof. (i) The first change to prove is that A_{12} in (1.5) is replaced by J in (3.3). This follows from the last part of Proposition 2.1.

The second addition to Theorem 1.1 in this context is inequality (3.5). To see this observe that the matrix $(E + \tau I)^{-1}J$ is skew-Hermitian with respect to the positive definite inner product $y^*(E + \tau I)x$, $x, y \in \mathbb{C}^n$. Hence, its eigenvalue condition number, with respect to the new inner

product, equals one. A standard inequality between the induced norms, as in Remark 2.3, finishes the proof.

(ii) It is enough to see that JQ is skew-Hermitian and RQ and E are positive semidefinite with respect to the new inner product. \square

Remark 3.4. Recall that the corresponding operator norm and adjoint of $X \in \mathbb{C}^{n,n}$ are given by

$$\|X\|_Q := \left\| Q^{1/2} X Q^{-1/2} \right\|, \quad X_Q^* = Q^{-*} X^* Q^*.$$

A dissipative Hamiltonian pencil arising from linearisation (see e.g. Subsection 5.3 below) shows that it is preferable to use these norms rather than the condition-number-based estimates in Remark 2.3.

4. PROOF OF THEOREM 1.2

In [6], Banks, Kulkarni, Mukherjee and Srivastava proved the following major result on estimating eigenvalue condition numbers. We present it here in a form adapted to our notation and purposes. Recall that if A has distinct eigenvalues $\lambda_1, \dots, \lambda_n$ and its spectral decomposition is given by $A = \sum_{i=1}^n \lambda_i v_i v_i^* = V D V^{-1}$ where $w_i^* v_i = 1$, then the *eigenvalue condition number* of λ_i is defined as

$$\kappa(\lambda_i, A) := \|v_i w_i^*\|.$$

Theorem 4.1. *Let $M \in \mathbb{C}^{n \times n}$ be a matrix with $\|M\| \leq 1$, and let $\tau \in (0, 1)$. Consider a complex Ginibre matrix G_n . With probability one, the perturbed matrix $M + \tau G_n$ has distinct eigenvalues, which we denote by $\lambda_1(\tau), \dots, \lambda_n(\tau)$. Then for every $r > 0$ we have*

$$\mathbb{E} \left[\sum_{|\lambda_i(\tau)| \leq r} \kappa(\lambda_i(\tau), M + \tau G_n)^2 \right] \leq \frac{n^2 r^2}{\tau^2}.$$

We are ready to prove the second result of the paper.

Proof of Theorem 1.2. Fix $\tau > 0$ for the whole proof. Observe that Theorem 4.1 bounds the expected value of a certain part of the sum $\sum_{i=1}^n \kappa(\lambda_i(\tau), M + \tau G_n)^2$. As the first step of the proof we derive an estimate of the expectation of the whole sum. For this consider the events

$$\begin{aligned} \Xi_t &:= \{t + 2\sqrt{2} < \|G_n\| \leq t + 1 + 2\sqrt{2}\}, \quad t = 0, 1, \dots, \\ \Xi_{-1} &:= \{\|G_n\| \leq 2\sqrt{2}\}. \end{aligned}$$

As $\tau, \|M\| \leq 1$, we have

$$|\lambda_i(\tau)| \leq \|M + \tau G_n\| \leq \|G_n\| + 1, \quad i = 1, \dots, n.$$

Hence, for $r = t + 2 + 2\sqrt{2}$ we have

$$\sum_{i=1}^n \kappa(\lambda_i(\tau), M + \tau G_n)^2 = \sum_{|\lambda_i(\tau)| \leq r} \kappa(\lambda_i(\tau), M + \tau G_n)^2 \quad \text{on the event } \Xi_t.$$

This gives the following bound for the conditional expectation

$$\mathbb{E} \left(\sum_{i=1}^n \kappa(\lambda_i(\tau), M + \tau G_n)^2 \mid \Xi_t \right) \leq \frac{n^2 (t + 2 + 2\sqrt{2})^2}{\tau^2}, \quad t = -1, 0, 1, \dots$$

By Lemma 2.2 of [6] we have $\mathbb{P}(\Xi_t) \leq 2e^{-nt^2}$, $t = 0, 1, \dots$. We estimate trivially $\mathbb{P}(\Xi_{-1})$ by 1. Altogether, we obtain

$$\begin{aligned}
\mathbb{E} \sum_{i=1}^n \kappa(\lambda_i(\tau), M + \tau G_n)^2 &\leq \sum_{t=-1}^{\infty} \mathbb{P}(\Xi_t) \frac{n^2(t+2+2\sqrt{2})^2}{\tau^2} \\
&\leq \frac{(9+4\sqrt{2})n^2}{\tau^2} + \frac{2n^2}{\tau^2} \sum_{t=0}^{\infty} e^{-nt^2} (t^2 + (4\sqrt{2}+4)t + 8\sqrt{2} + 12) \\
&\leq \frac{n^2}{\tau^2} \left(9 + 4\sqrt{2} + 24 + 16\sqrt{2} + 2 \int_0^{\infty} e^{-nt^2} (t^2 + (4\sqrt{2}+4)t + 8\sqrt{2} + 12) dt \right) \\
&\leq \frac{n^2}{\tau^2} \left(33 + 20\sqrt{2} + \frac{\sqrt{\pi}}{2n^{3/2}} + \frac{4\sqrt{2}+4}{n} + \frac{\sqrt{\pi}(8\sqrt{2}+12)}{n^{1/2}} \right) \\
&=: \frac{\beta(n)}{\tau^2}.
\end{aligned}$$

Recall that the condition number of individual eigenvalues bounds the eigenvalue condition number κ_V (see, e.g., Lemma 3.1 of [6]), hence

$$\mathbb{E}(\kappa_V(M + \tau G_n)) \leq \mathbb{E} \sqrt{n \sum_{i=1}^n \kappa(\lambda_i(\tau), M + \tau G_n)^2} \quad (4.1)$$

$$\leq \sqrt{n \mathbb{E} \sum_{i=1}^n \kappa(\lambda_i(\tau), M + \tau G_n)^2} \quad (4.2)$$

$$\leq \frac{\sqrt{n\beta(n)}}{\tau} =: \frac{\alpha(n)}{\tau}. \quad (4.3)$$

Note that, by its definition, $\alpha(n)$ has the following large n asymptotics

$$\lim_{n \rightarrow \infty} \frac{\alpha(n)}{n^{3/2}} \leq \sqrt{33 + 20\sqrt{2}} < 7.82843.$$

We prove now (1.7). Recall that $\tau > 0$ is fixed and both matrices $M + \tau G_n$ and $M + \Delta + \tau G_n$ are almost surely diagonalizable. Let \hat{G}_n be a sample of the Ginibre ensemble for which this happens. Let μ_0 be the eigenvalue of $M + \Delta + \tau \hat{G}_n$ of minimal absolute value. By the Bauer-Fike theorem [7], there exists an eigenvalue λ_0 of $M + \tau \hat{G}_n$ with $|\lambda_0 - \mu_0| \leq \|\Delta\| \kappa_V(M + \tau \hat{G}_n)$. Hence,

$$|\lambda_0| - \|\Delta\| \kappa_V(M + \tau \hat{G}_n) < |\mu_0|.$$

Returning to random variables, we have almost surely that

$$\min_{i=1, \dots, n} |\lambda_i(\tau)| - \|\Delta\| \kappa_V(M + \tau G_n) \leq \min_{i=1, \dots, n} |\lambda_i^\Delta(\tau)|.$$

Employing (4.3) we receive

$$\mathbb{E} \min_{i=1, \dots, n} |\lambda_i(\tau)| - \mathbb{E} \min_{i=1, \dots, n} |\lambda_i^\Delta(\tau)| \leq \frac{\|\Delta\| \alpha(n)}{\tau}.$$

By symmetry of the roles of M and $M + \Delta$, the formula (1.7) is proved. \square

5. PRACTICAL IMPLEMENTATIONS

In this section, we demonstrate the two main theorems of the paper applied to a collection of benchmark examples commonly studied in the literature. The results are collected in Figure 1 for a direct side-by-side comparison. The rows correspond to the individual examples described below, while the columns represent the two proposed methods.

Code and data for reproducing the numerical experiments, including implementations of both methods, are available online at https://github.com/hblazhko/index_detection. The code also supports custom configurations for additional experiments.

Remark 5.1. First method of index detection. The plots in the left column of Figure 1 refer to Theorem 1.1. They show the reciprocal $1/|\lambda(\tau)|$ vs. τ in blue. The parameter τ ranges from 10^{-20} to 10^2 in all examples. The reciprocal is computed as the smallest absolute value of the eigenvalues of the reversal pencil, due to numerical reasons. The slope of the line should be $1/2$ for index 2 (with no simple eigenvalues infinity) and 1 for index 1.

Furthermore, the plots show the reciprocals of the bounds (1.5), displayed as orange dash-dot lines (in some cases a different estimate is used, see below for details). Note that for some values of τ the lower bound in (1.5) might be negative, hence trivial. In such cases there is no upper bound on the left plot. Further, the parameters δ and τ_0 are marked with vertical lines (dashed purple and dotted red, respectively).

Remark 5.2. Second method of index detection. The plots in the right column of Figure 1 refer to Theorem 1.2. Solid blue lines show the smallest absolute value of the eigenvalues of

$$\frac{(E - hA)^{-1}(E + hA) + I}{\|(E - hA)^{-1}(E + hA) + I\|} + \tau G_n,$$

averaged over 10 samples of the complex Ginibre ensemble G_n , cf. Theorem 1.2. The slope of the line should be $1/2$ for index 2 (with no simple eigenvalues infinity) and 1 for index 1.

The plots additionally show the upper and lower bounds provided by Theorem 1.2 with $\|\Delta\| \leq e^{-15}$, indicated by green dash-dot lines. Observe a visible turning point in the log-log plot, after which the three curves begin to coincide. In particular, to the left of this point the calculated slope of the convergence may be inaccurate due to possible numerical errors. To the right of the turning point, the eigenvalues of the randomized matrix are computed accurately enough to estimate their slope.

5.1. Toy model. Consider pencil of the form $\lambda E - (J - R)$ with

$$E = \begin{bmatrix} I_n & 0 \\ 0 & 0 \end{bmatrix} \in \mathbb{C}^{2n, 2n}, \quad A = \begin{bmatrix} \frac{R_0 R_0^*}{\|R_0\|^2} & -J_0^* \\ J_0 & 0 \end{bmatrix}. \quad (5.1)$$

Note that for an invertible J_0 we have a regular pencil of index 2. In our experiments, we sampled J_0 and R_0 as real 100×100 matrices with i.i.d. normal entries. In particular, both matrices were invertible almost surely.

The numerical results are presented in Figure 1. Both plots clearly exhibit regions of τ with convergence rate $1/2$, indicating the presence of a Kronecker block of size two.

The bounds shown for Method 1 are derived from Theorem 1.1 with $\delta = e^{-15}$. In this case, the parameter τ_0 from (1.3) exceeds 100, implying that the bounds are valid throughout the entire displayed range of τ . As one can observe, the lower bound closely follows the computed smallest eigenvalue over a certain interval and exhibits the same slope $1/2$. The upper bound initially displays similar behavior; however, it loses accuracy earlier and begins to deviate once the lower bound in Theorem 1.1 becomes negative.

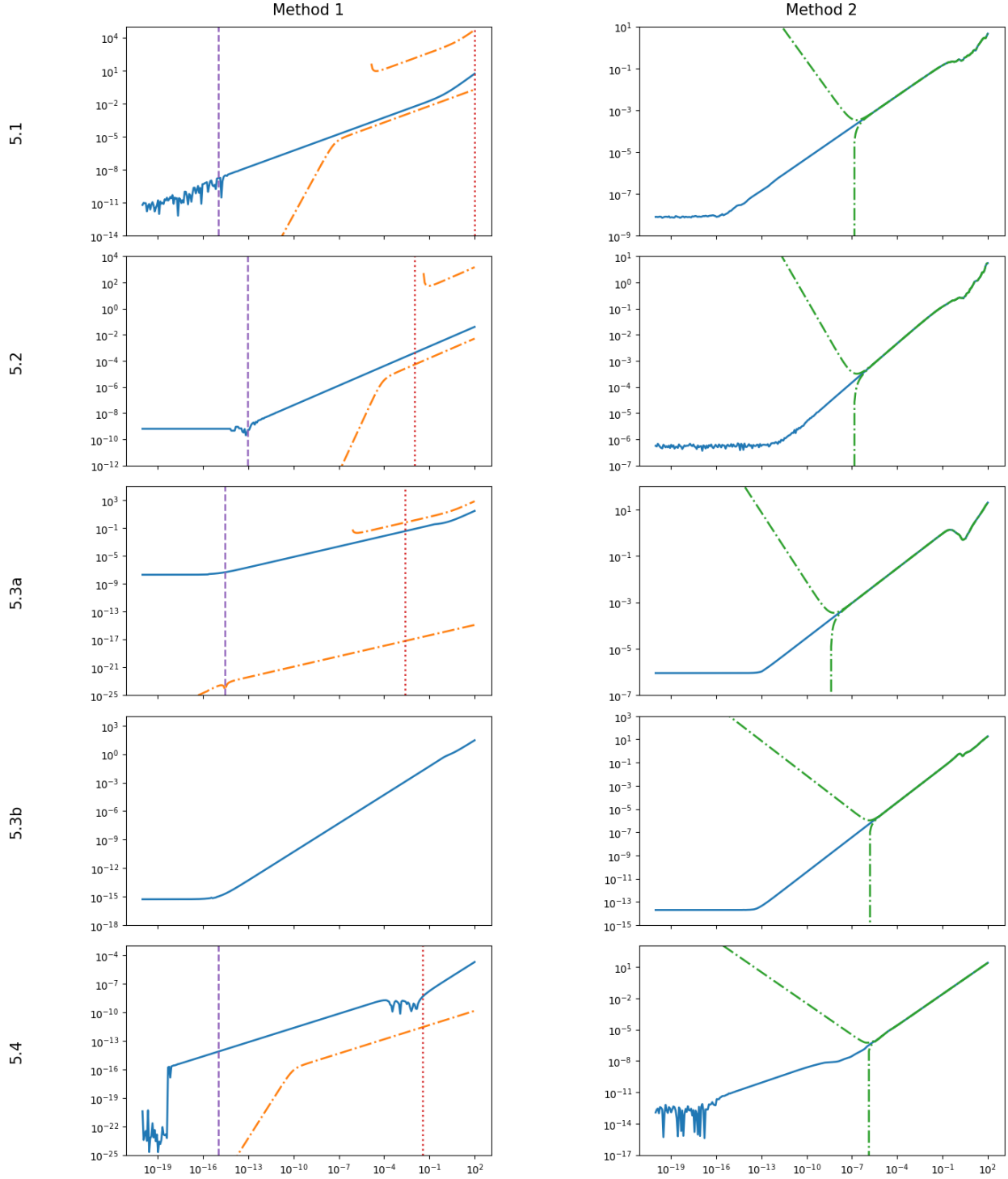


FIGURE 1. The plots show the reciprocals of eigenvalues corresponding to Theorem 1.1 (left column, solid blue line) and the eigenvalues corresponding to Theorem 1.2 (right column, solid blue line). The corresponding bounds are shown with dash-dot orange lines. See Remarks 5.1 and 5.2 for a detailed description. The rows correspond to the subsections, as indicated.

In this model both methods give accurate plots for recognizing the index, which is confirmed by theoretical bounds from Theorem 1.1 and 1.2, respectively.

5.2. The influence of a congruence transformation. The purpose of this example is to illustrate how the accuracy of the bounds provided in Theorem 1.1 degrades without the knowledge of the explicit block structure (2.1). Let us consider the same pencil (5.1) from Subsection 5.1 but transform it with a congruence matrix S sampled as a real 100×100 matrix with i.i.d. standard normal entries:

$$S(\lambda E - (J - R))S^*. \quad (5.2)$$

Note that the numerically computed eigenvalues $s_1 \geq \dots \geq s_{200}$ of (positive semidefinite) SES^* are of magnitude $s_{100} \simeq 10^1$, while $s_{101} \simeq 10^{-13}$. Therefore, transforming it into the structure (2.1) would require a rank decision. However, both plots of the eigenvalues shown in Figure 1 do not differ qualitatively from the plot corresponding to the previous case $S = I$ and the index 2 structure is well recognized without the rank decision process. The latter is needed only for plotting the bounds from Theorem 1.1. If we interpret

$$E = U \operatorname{diag}(s_1, \dots, s_{100}, 0, \dots, 0)U^*, \quad \Delta_E = U \operatorname{diag}(0, \dots, 0, s_{101}, \dots, s_{200})U^*,$$

where U is the eigenvector matrix of E , we have $\delta = s_{101} \simeq 10^{-13}$ and $\tau_0 \approx 0.0106$.

In this model both methods give accurate plots for recognizing the index, which is confirmed by theoretical bounds from Theorem 1.1 and 1.2, respectively.

5.3. A dissipative Hamiltonian linearisation of a system of vibrating strings. Consider the quadratic polynomial $\lambda^2 M + \lambda C + K$ arising from the mass-spring-damper system described in [35, Section 3.9]. The coefficients have the form

$$\begin{aligned} M &= \operatorname{diag}(m_1, \dots, m_n), \\ C &= P \operatorname{diag}(d_1, \dots, d_{n-1}, 0) P^\top + \operatorname{diag}(t_1, \dots, t_n), \\ K &= P \operatorname{diag}(k_1, \dots, k_{n-1}, 0) P^\top + \operatorname{diag}(\kappa_1, \dots, \kappa_n), \text{ with} \\ P &= [\delta_{ij} - \delta_{i,j+1}]_{i,j=1}^n. \end{aligned}$$

The corresponding port-Hamiltonian linearization is of the form

$$E = \begin{bmatrix} M & 0 \\ 0 & I \end{bmatrix}, \quad R = \begin{bmatrix} C & 0 \\ 0 & 0 \end{bmatrix}, \quad J = \begin{bmatrix} 0 & -I_n \\ I_n & 0 \end{bmatrix}, \quad Q = \begin{bmatrix} I_n & 0 \\ 0 & K \end{bmatrix}.$$

Case a) The theory developed in [27] allows us to identify a set of parameters for which the above polynomial lies in a neighborhood of index 2 polynomials, while remaining relatively far from singular polynomials. Specifically, we can set $m_1 = d_1 = t_1 = \varepsilon \ll 1$, while keeping the remaining coefficients separated from zero. By [27] we obtain in this way a pencil close to index 2, however, in a safe distance from the set of singular pencils.

Figure 1, row 5.3a, presents both methods applied to the case of $n = 10$ strings with $\varepsilon = e^{-15}$. The bounds shown for Method 1 are obtained from Corollary 3.3(ii) for port-Hamiltonian pencils with $Q > 0$, where δ is taken equal to $3\varepsilon = 3e^{-15}$. In this case, τ_0 from (1.3) equals approximately 0.002.

Case b) On the other hand, setting $m_1 = \varepsilon \ll 1$ while keeping d_1 and t_1 bounded away from zero leads to pencil close to index 1, in a safe distance from the set of singular pencils and pencils of index 2.

Figure 1, row 5.3b, shows both methods applied to the case of $n = 10$ strings with $\varepsilon = e^{-15}$. Since the resulting pencil is of index 1, the bounds provided for Method 1 are not applicable in this setting. Nevertheless, both plots clearly exhibit a convergence rate equal to 1.

In this model both methods give accurate plots for recognizing the index, confirmed by Theorems 1.1, and Theorem 1.2, respectively. Thus, a clear distinction between pencils near to index 1 and near to index 2 is visible, even though the perturbed pencil (for which the eigenvalues were computed) has no eigenvalue at infinity.

5.4. Electrical circuit. Consider the two-stage CMOS operational amplifier introduced in [31] and later studied from the numerical point of view in [13]. The associated matrix pencil has an infinite eigenvalue of algebraic multiplicity 6 and is of index 2.

The numerical problem arising in this example is that the nonzero entries of E and A are of magnitude 10^{-14} and 10^{-4} , respectively, which is too small to obtain the desired convergence for τ ranging from 10^{-20} to 10^2 . To keep τ in the same range in all examples we multiply both matrices by e^{10} . Both plots presented in Figure 1 show convergence rate $1/2$ for a certain range of τ . Furthermore, τ_0 marked on the plot corresponds in this situation to the place where the smallest eigenvalue (of the reversal pencil) arising from the origin, interferes with other eigenvalues, as visible on the plot.

In this example both Methods produce a clear recognition of index 2. Further, Method 1 is confirmed by theoretical bounds. Moreover, in this example the theoretical bounds from Theorem 1.2 lose their accuracy due to the different magnitudes of A and E .

5.5. Errors in the staircase form. In practice, the matrix E is typically diagonal, and hence its kernel is clearly identified. The difficulty in determining whether a system is of index 2 lies in verifying whether the matrix A_{22} in the block form (2.1) is a zero matrix. To highlight this, we examine how perturbations in the matrix A affect the behavior of the eigenvalues and the bounds in Theorem 1.1. To this end, we consider the pencil (5.1) from Subsection 5.1, perturbed by a small matrix Δ_A .

Figure 2 shows Method 1 applied to the pencil perturbed by a matrix Δ_A sampled as a 200×200 matrix with i.i.d. real Gaussian entries of variance e^{-7} , e^{-5} , and e^{-3} (from left to right, respectively). The displayed bounds are obtained from Corollary 2.2 for the case $\Delta_E = 0$, with $\delta = e^{-7}, e^{-5}, e^{-3}$, respectively.

Note that the estimates in Corollary 2.2 hold for $\tau > 0$, not only $\tau > \delta$, which was previously the case. Hence, the value of δ is not marked on the plot. In all cases τ_0 exceeds 100 so the obtained bounds are meaningful on the whole considered range of τ , thus it is not marked as well.

Although the pencil (5.1) is of index 2, larger perturbation magnitudes lead to wider regions in which the convergence rate equals 1, corresponding to pencils of index 1. In particular, this correspondence allows one to estimate the distance to the set of index 2 pencils via the observed convergence behavior. We also note that, in this example, the provided bounds are nearly sharp for $\delta = e^{-3}$.

One can observe that the range of values of τ can be divided into four distinct regions.

- (I) Too large values of τ (relative to the scale of E, A), where the statement is not yet valid and its effect cannot be observed;
- (II) Optimal values, where the convergence rate given in the Puiseux expansion (1.1) can be observed;
- (III) Suboptimal values of τ , i.e., values for which the numerics change a Kronecker block of size 2 into two blocks of size 1;
- (IV) Too small values of τ , for which round-off error effects hinder any computation.

6. CONCLUSIONS

We have answered questions (Q1) and (Q2) positively. We have demonstrated, both theoretically and numerically, that the second order Kronecker blocks are visible and detectable in the expansion

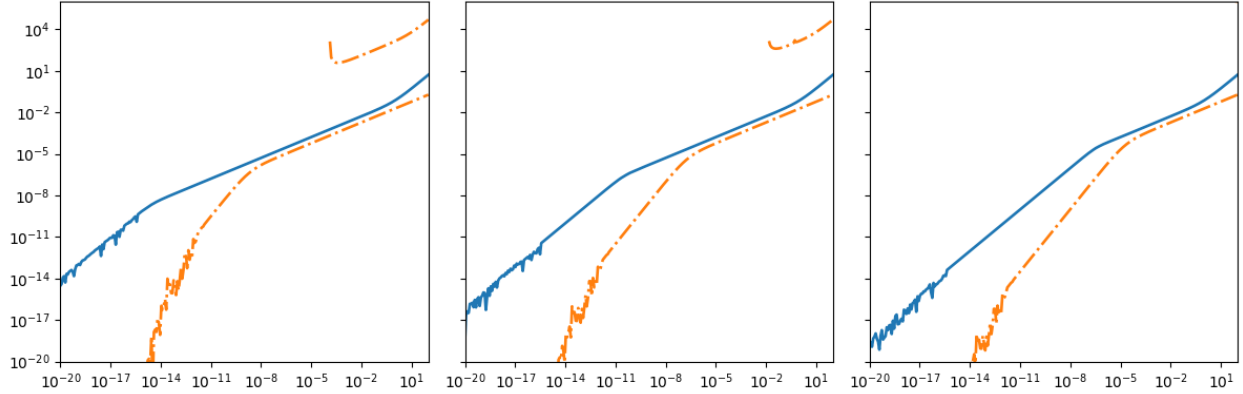


FIGURE 2. The plots show the reciprocals of eigenvalues corresponding to Theorem 1.1 with solid blue lines. Corresponding bounds are shown with dash-dot orange lines. See Remark 5.1 for a full description. The plots correspond to the variance e^{-7} , e^{-5} , e^{-3} of the entries of Δ_A from Subsection 5.5, respectively.

of eigenvalues. Furthermore, the Cayley transform preserves this feature despite the numerical error. We have provided heuristic evidence addressing question (Q3).

7. ACKNOWLEDGMENTS

Hanna Blazhko gratefully acknowledges the support of the program Excellence Initiative – Research University at the Jagiellonian University in Kraków.

REFERENCES

- [1] Sk Safique Ahmad, Rafikul Alam, and Ralph Byers. On pseudospectra, critical points, and multiple eigenvalues of matrix pencils. *SIAM Journal on Matrix Analysis and Applications*, 31(4):1915–1933, 2010.
- [2] Richard O Akinola, Melina A Freitag, and Alastair Spence. The calculation of the distance to a nearby defective matrix. *Numerical Linear Algebra with Applications*, 21(3):403–414, 2014.
- [3] R. Alam and S Bora. On sensitivity of eigenvalues and eigendecompositions of matrices. *Linear Algebra and its applications*, 396:273–301, 2005.
- [4] Rafikul Alam. On the construction of nearest defective matrices to a normal matrix. *Linear algebra and its applications*, 395:367–370, 2005.
- [5] Rafikul Alam, Shreemayee Bora, Ralph Byers, and Michael L Overton. Characterization and construction of the nearest defective matrix via coalescence of pseudospectral components. *Linear Algebra and its Applications*, 435(3):494–513, 2011.
- [6] Jess Banks, Archit Kulkarni, Satyaki Mukherjee, and Nikhil Srivastava. Gaussian regularization of the pseudospectrum and davis’ conjecture. *Communications on Pure and Applied Mathematics*, 74(10):2114–2131, 2021.
- [7] Friedrich L Bauer and Charles T Fike. Norms and exclusion theorems. *Numerische mathematik*, 2(1):137–141, 1960.
- [8] Fernando De Terán, Froilán M Dopico, and Julio Moro. First order spectral perturbation theory of square singular matrix pencils. *Linear algebra and its applications*, 429(2-3):548–576, 2008.
- [9] Etienne Emmrich and Volker Mehrmann. Operator differential-algebraic equations arising in fluid dynamics. *Computational Methods in Applied Mathematics*, 13(4):443–470, 2013.
- [10] Mehmet Erbay, Birgit Jacob, Kirsten Morris, Timo Reis, and Caren Tischendorf. Index concepts for linear differential-algebraic equations in infinite dimensions. *DAE Panel*, 2, 2024.
- [11] Timm Faulwasser, Bernhard Maschke, Friedrich Philipp, Manuel Schaller, and Karl Worthmann. Optimal control of port-Hamiltonian descriptor systems with minimal energy supply. *SIAM Journal on Control and Optimization*, 60(4):2132–2158, 2022.
- [12] Roland W Freund and Florian Jarre. An extension of the positive real lemma to descriptor systems. *Optimization methods and software*, 19(1):69–87, 2004.

- [13] Hannes Gernandt and Carsten Trunk. Eigenvalues of parametric rank-one perturbations of matrix pencils. *Linear Algebra and its Applications*, 708:429–457, 2025.
- [14] Mark Giesbrecht, Joseph Haraldson, and George Labahn. Computing the nearest rank-deficient matrix polynomial. In *Proceedings of the 2017 ACM International Symposium on Symbolic and Algebraic Computation*, pages 181–188, 2017.
- [15] Nicolas Gillis, Volker Mehrmann, and Punit Sharma. Computing the nearest stable matrix pairs. *Numerical Linear Algebra with Applications*, 25(5):e2153, 2018.
- [16] Nicolas Gillis and Punit Sharma. Finding the nearest positive-real system. *SIAM Journal on Numerical Analysis*, 56(2):1022–1047, 2018.
- [17] Nicolas Gillis and Punit Sharma. Solving matrix nearness problems via Hamiltonian systems, matrix factorization, and optimization. In *Recent Stability Issues for Linear Dynamical Systems: Cetraro, Italy 2021*, pages 1–83. Springer, 2024.
- [18] Michiel E Hochstenbach, Christian Mehl, and Bor Plestenjak. Solving singular generalized eigenvalue problems by a rank-completing perturbation. *SIAM Journal on Matrix Analysis and Applications*, 40(3):1022–1046, 2019.
- [19] Michiel E. Hochstenbach, Christian Mehl, and Bor Plestenjak. Solving singular generalized eigenvalue problems. Part II: Projection and augmentation. *SIAM Journal on Matrix Analysis and Applications*, 44(4):1589–1618, 2023.
- [20] Paul Kotyczka and Tobias Thoma. Symplectic discrete-time energy-based control for nonlinear mechanical systems. *Automatica*, 133:109842, 2021.
- [21] Daniel Kressner and Bor Plestenjak. Analysis of eigenvalue condition numbers for a class of randomized numerical methods for singular matrix pencils. *BIT Numerical Mathematics*, 64(3), 2024.
- [22] Daniel Kressner and Ivana Šain Glibić. Singular quadratic eigenvalue problems: Linearization and weak condition numbers. *BIT Numerical mathematics*, 63(1):18, 2023.
- [23] Daniel Kressner and Matthias Voigt. Distance problems for linear dynamical systems. In *Numerical algebra, matrix theory, differential-algebraic equations and control theory: Festschrift in honor of Volker Mehrmann*, pages 559–583. Springer, 2015.
- [24] V. B. Lidskii. Perturbation theory of non-conjugate operators. *Zh. Vychisl. Mat. Mat. Fiz.*, 6(1):52–60, 1966. Translated in *U.S.S.R. Comput. Math. Math. Phys.*, 6(1):73–85, 1966.
- [25] D Steven Mackey, Niloufer Mackey, Christian Mehl, and Volker Mehrmann. Möbius transformations of matrix polynomials. *Linear Algebra and its Applications*, 470:120–184, 2015.
- [26] C. Mehl, V. Mehrmann, and M. Wojtylak. Linear algebra properties of dissipative Hamiltonian descriptor systems. *SIAM Journal on Matrix Analysis and Applications*, 39(3):1489–1519, 2018.
- [27] C. Mehl, V. Mehrmann, and M. Wojtylak. Distance problems for dissipative Hamiltonian systems and related matrix polynomials. *Linear algebra and its applications*, 623:335–366, 2021.
- [28] Christian Mehl, Volker Mehrmann, and Michał Wojtylak. Matrix pencils with coefficients that have positive semidefinite Hermitian parts. *SIAM Journal on Matrix Analysis and Applications*, 43:1186–1212, 2022.
- [29] Volker Mehrmann and Benjamin Unger. Control of port-hamiltonian differential-algebraic systems and applications. *Acta Numerica*, 32:395–515, 2023.
- [30] Jens Saak and Matthias Voigt. Model reduction of constrained mechanical systems in MM. ESS. *IFAC-PapersOnLine*, 51(2):661–666, 2018.
- [31] Ralf Sommer, Dominik Krauß, Eric Schäfer, and Eckhard Hennig. Application of symbolic circuit analysis for failure detection and optimization of industrial integrated circuits. In *Design of Analog Circuits through Symbolic Analysis*, pages 445–477. Bentham Science Publishers, 2012.
- [32] Gilbert W Stewart. On the sensitivity of the eigenvalue problem $Ax = \lambda Bx$. *SIAM Journal on Numerical Analysis*, 9(4):669–686, 1972.
- [33] Gilbert W Stewart and Ji-guang Sun. *Matrix perturbation theory*. Academic Press, new York, 1990.
- [34] Ji-guang Sun. Perturbation expansions for invariant subspaces. *Linear Algebra and its Applications*, 153:85–97, 1991.
- [35] F. Tisseur and K. Meerbergen. The quadratic eigenvalue problem. *SIAM Review*, 43:235–286, 2001.
- [36] Paul Van Dooren. The computation of Kronecker’s canonical form of a singular pencil. *Linear Algebra and its Applications*, 27:103–140, 1979.
- [37] J. H. Wilkinson. Kronecker’s canonical form and the QZ algorithm. *Linear Algebra and its Applications*, 28:285–303, 1979.